Electronic Supplementary Information

Fibre Optic ATR-IR Spectroscopy at Cryogenic Temperatures: In-Line Reaction Monitoring on Organolithium Compounds

Daniel Lumpi*, Christoph Wagner, Matthias Schöpf, Ernst Horkel, Georg Ramer, Bernhard Lendl, and Johannes Fröhlich*

[a] Institute of Applied Synthetic Chemistry, [b] Institute of Chemical Technologies and Analytics

Table of Contents:

1. Experimental Parameter

The ATR fibre system consisted of a Bruker Matrix F FTIR spectrometer connected to an ATR fibre probe (A.R.T. Photonics, Berlin; Ø 12 mm) and a MCT (mercury cadmium telluride) detector (Belov Technology, Co.,Inc.). The ATR sensor probe comprised two 1 m long silver halide fibres (Ø 1 mm) connected to a conical two bounce diamond ATR element attached to the endface of a rod-shaped hastelloy housing. The optical interfacing to the spectrometer was achieved *via* off-axis parabolic mirrors focussing the IR beam onto the first light guide and collecting the light from the second fibre; for more information on the optical setup, see the section 2 (ESI). Spectra were recorded over the duration of the entire reaction at a spectral resolution of 4 cm^{-1}, averaging 24 scans at a scanner velocity setting of 40 kHz yielding a temporal resolution of 10 s. To achieve a higher time resolution of 4 s for following the formation and consumption of the reaction intermediates (**2** and **3**) more in detail, the number repetitive scans was reduced to 10. The relative amount of formed Li-species (100 % - indicated in the graphs for the formation of organolithium compounds) does not necessarily equals full conversion but clearly indicates the end of the reaction.

The fibre probe was mounted through a ground neck into a 100 mL 4-neck round bottom flask equipped with a thermometer, an argon inlet and a septum. The reaction vessel was charged with dry solvent (THF, Et$_2$O, 20 mL) and cooled *via* a cooling bath. For this purpose a dewar was charged depending on reaction temperature: acetone/N$_{2(l)}$ slush for -86 °C, chlorobenzene/N$_{2(l)}$ slush for -40 °C, H$_2$O/ice mixture for 2 °C and H$_2$O for ambient temperature. After a steady temperature in the vessel was reached a background spectrum was recorded, the measurement started and the lithium species (5.0 mmol, 1.0 equiv. of 2.0 M *n*BuLi in cyclohexane obtained from Sigma Aldrich or freshly prepared LDA[3]) added. Subsequently the respective reactant (5.0 mmol, 1.0 equiv., from commercial sources) was rapidly added *via* a syringe.

Investigations concerning an organolithium intermediates (**2** and **3**) were realised charging the flask with 5,5'-dibromo-2,2'-bithiophene[2] **1** (486 mg, 5.0 mmol, 1.0 equiv.) and dry THF (15 mL). At -40 °C a pre-cooled LDA solution (-40 °C) was added *via* syringe under argon atmosphere. After a reaction time of 20 min quenching with an excess of methanol, standard workup and column chromatography (PE) afforded 4,4'-dibromo-2,2'-bithiophene **4** (418 mg) in 86 % yield.[3]

---

1   LDA was separately prepared from diisopropylamine (5.0 mmol, 1.0 equiv.) and 2.0 M *n*BuLi (5.0 mmol, 1.0 equiv.) in 2.5 mL of the corresponding solvent at 0 °C under argon.

2   N.-X. Wang, *Synth. Commun.* **2003**, *33 (12)*, 2119.

3   Physical data in agreement with published values; see R. Bobrovsky, C. Hametner, W. Kalt and J. Froehlich, *Heterocycles*, 2008, **76 (2)**, 1249.

2. Instrumental Setup

Figure 2.1 shows the experimental setup of the ATR-IR fibre probe.
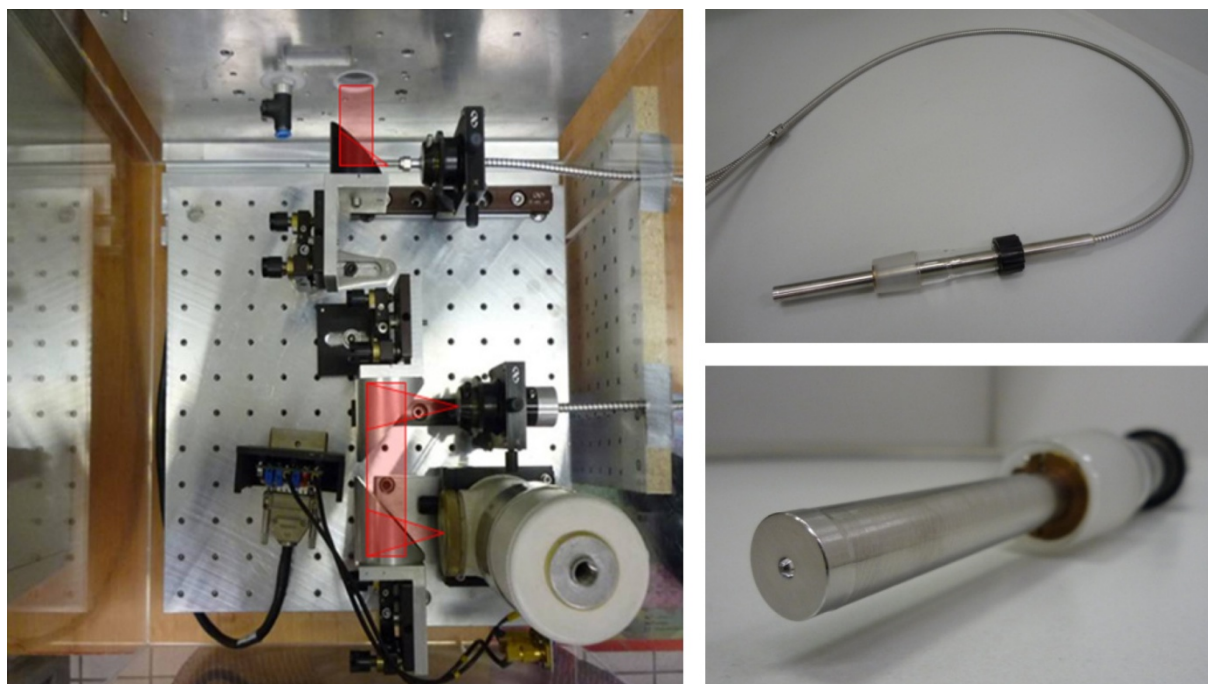
Figure 2.1. Optical path in the experimental setup (left); IR fibre optic and ATR-IR probe (right).

3. Fast Fourier Transformation (FFT) Correction

In this chapter we demonstrate a typical example of an FFT correction starting from spectral raw data acquired in a reaction of bromobenzene and *n*BuLi in THF at -86 °C. In the course of the correction procedure Fourier coefficients in the linear combination are successively set to zero which reduces artificially introduced fringes in the spectra significantly (figures 3.1-3.11). In detail, the fringes in the spectra were removed by performing a fast Fourier transform (FFT) on the spectra, then setting the first few Fourier components (as indicated in figure 3.1) to zero and finally applying the inverse FFT to achieve the corrected spectra. The exact number of low frequency Fourier components to set to zero was determined manually, by increasing the number of removed components until the fringes strongly attenuated but distortion in the spectra was not noticeable.

An introduction to FFT filtering techniques (including the mathematical fundamentals) can be found in "Introduction to Signal Processing" by Orphanidis, Sophocles J.[4] In our work FFT was used to implement a high pass filter with a rectangular window function, meaning slow changes in the spectra, such as the fringes, were attenuated. The spectra were transformed from the frequency domain to the spatial domain and then multiplied with a rectangular function that equals zero for all lengths below and including the cutoff length and equals one everywhere else. The cutoff length (l) is related to the number of components set to zero by the following equation:

$$l=(k-1)/(N*r)$$

l... cutoff length

k... last point in the interferogram set to zero

N... number of datapoints in the spectrum

r... distance of datapoints in wavenumbers

This correction procedure quantitatively removes introduced fringes up to temperature deviations of approximately 7-10 °C. Higher temperature deviations result in residual fringes in the spectra after correction.

---

4   S. J. Orfanidis, *Introduction to Signal Processing*, Sophocles J. Orfanidis, 2010.

Figure 3.1 shows the FFT procedure performed one single spectrum at a reaction time of 40 s during the aforementioned metal halogen exchange reaction. As obvious from figure 3.1 (and 3.2 – 3.11) the fringes are largely reduced at the 8th level (0.00583 cm) of the correction. The enlarged image details show the effect of the FFT procedure on frequency and absorption values of significant bands (more details regarding these potential errors are given in subsection 3.1).
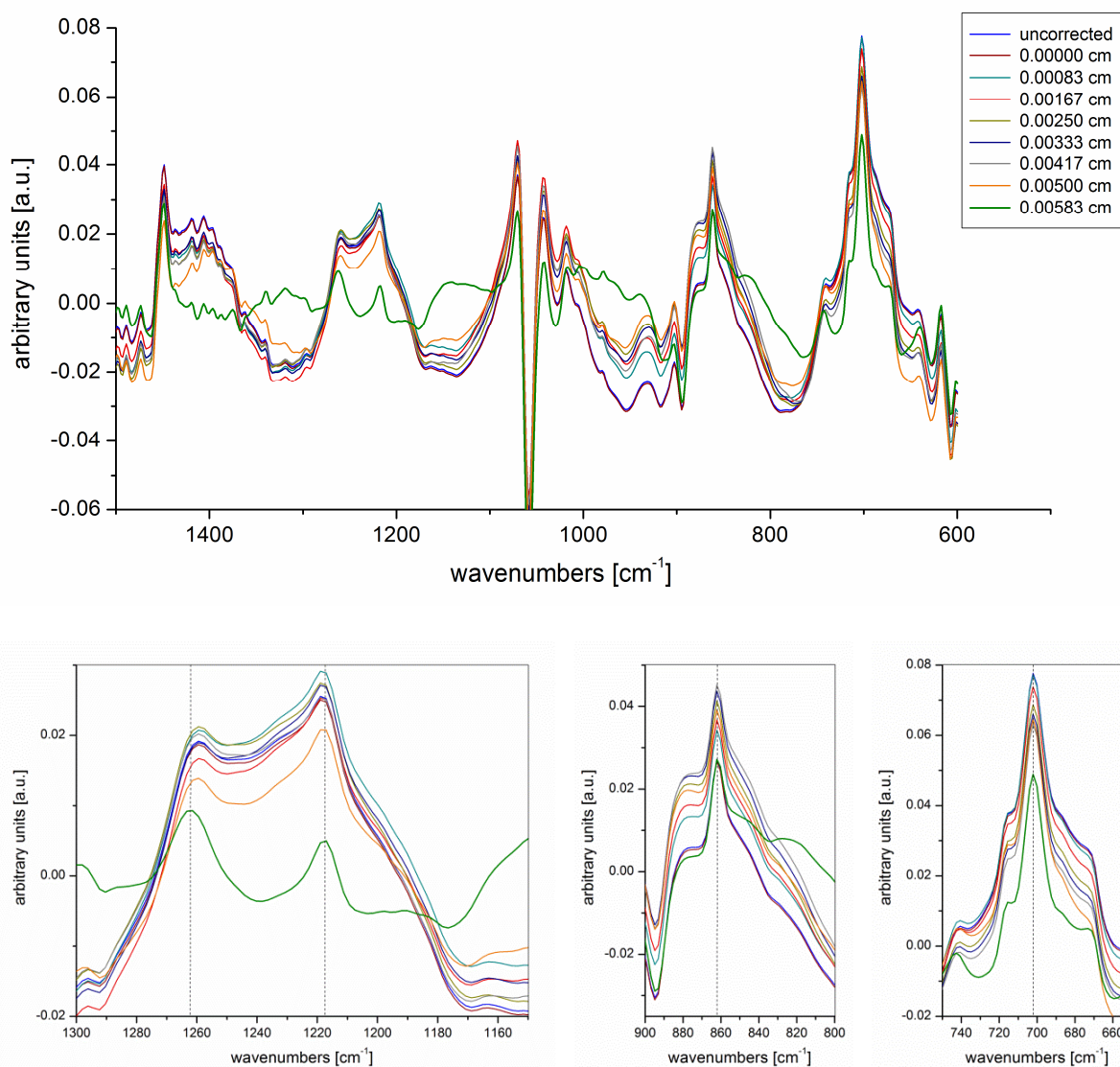
Figure 3.1. FFT correction performed on one single spectrum at 40 s in the reaction of bromobenzene and *n*BuLi in THF at -86 °C. This spectrum was treated with the FFT high pass filter at different cutoff lengths (l) of the rectangular window (as indicated in the legend). Enlarged image details for significant bands during the correction are shown in the lower section of the figure.

The effects of the FFT correction on the entire dataset during the reaction monitoring are illustrated in figures 3.2 – 3.10. Figure 3.11 shows the integration limits at an intense absorption of the formed phenyllithium; the results of this integration are given in figure 4.2 in the ESI.
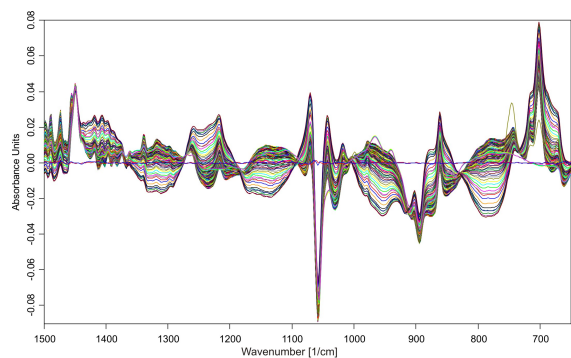
Figure 3.2. no correction; raw spectral data.
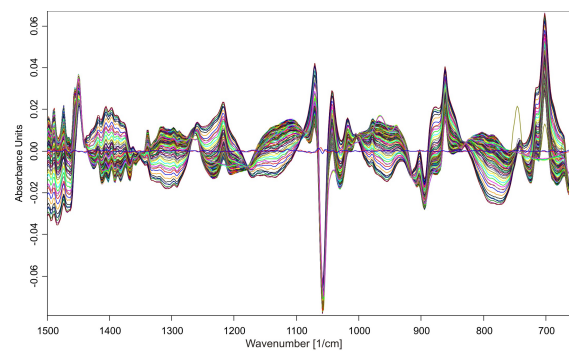
Figure 3.6. 4th level of FFT correction (0.00250 cm).
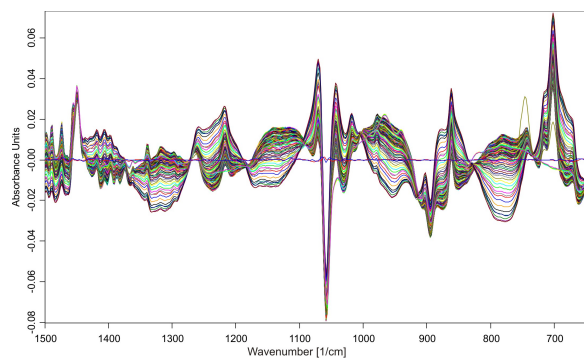
Figure 3.3. 1st level of FFT correction (0.00000 cm).
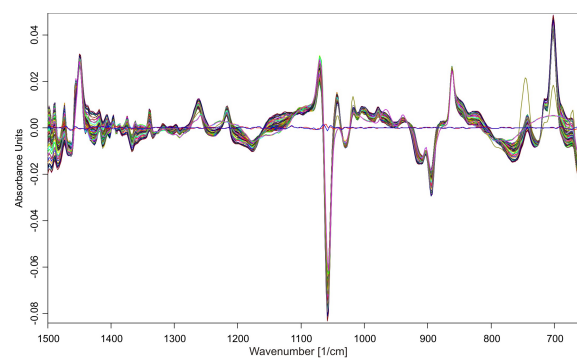
Figure 3.7. 5th level of FFT correction (0.00333 cm).
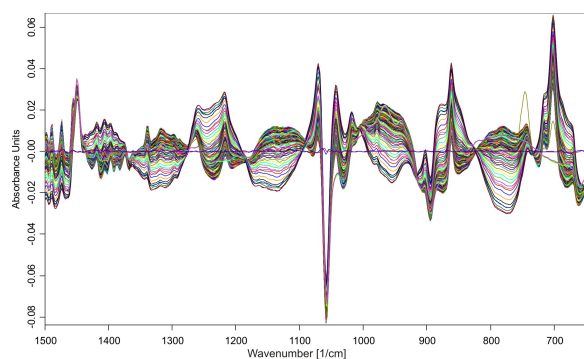
Figure 3.4. 2nd level of FFT correction (0.00083 cm).
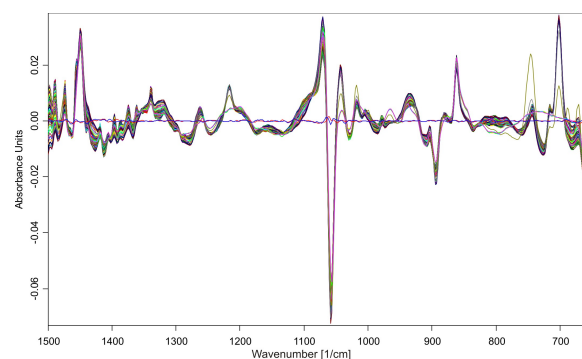
Figure 3.8. 6th level of FFT correction (0.00417 cm).
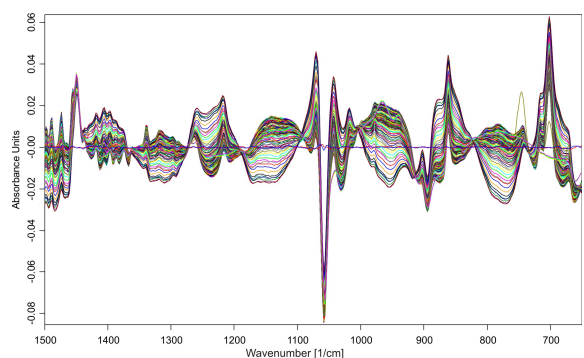
Figure 3.5. 3rd level of FFT correction (0.00167 cm).
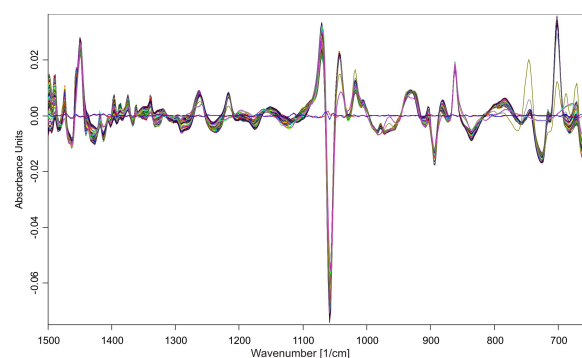
Figure 3.3. 7th level of FFT correction (0.00500 cm).
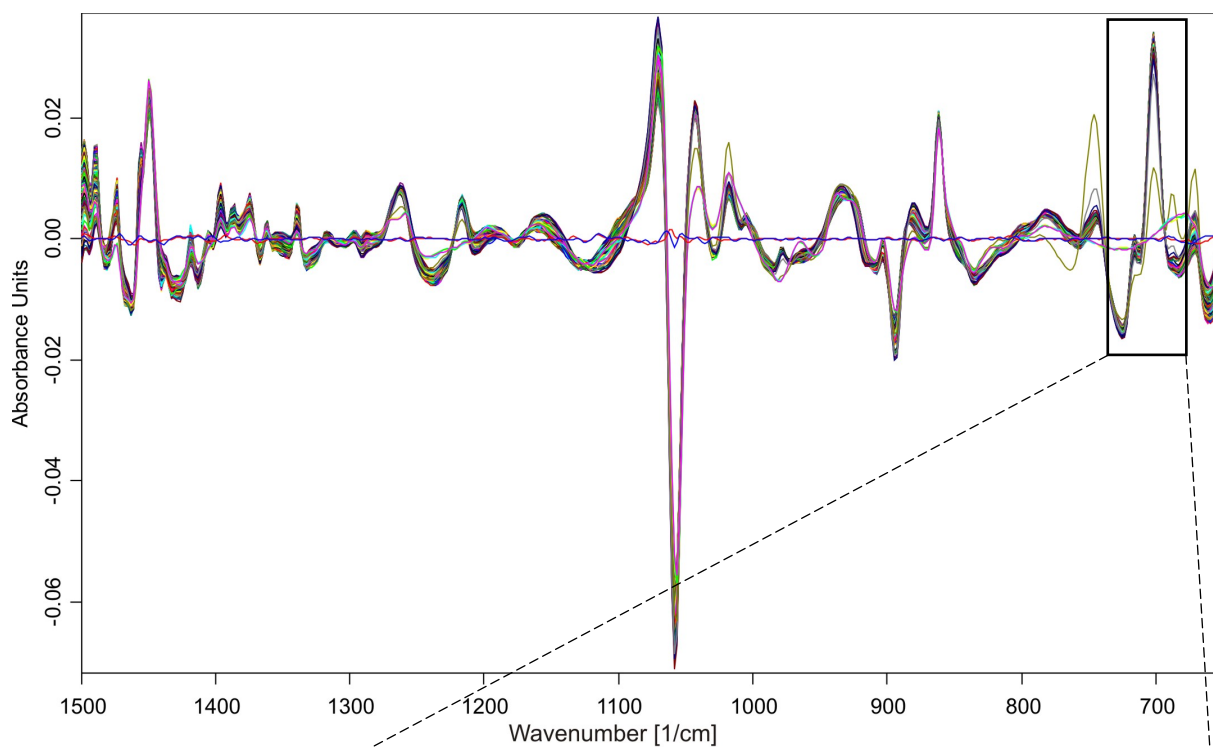
Figure 3.10. 8th level of FFT correction (0.00583 cm); fringes are significantly reduced.
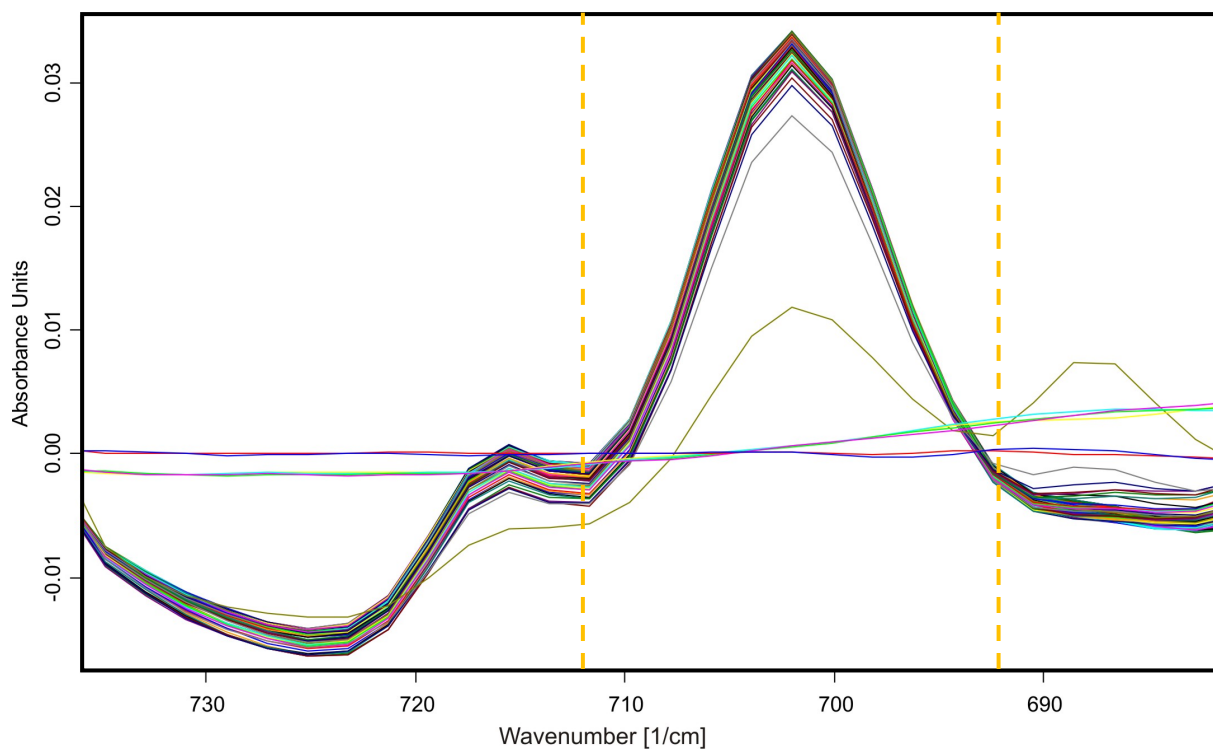
Figure 3.11. 8th level of FFT correction enlarged; dashed lines show the integration limits (~692 – ~712 cm^{-1}).

3.1. Potential Errors during the FFT Correction

The rectangular window function is known to cause distortions in the treated spectra[4]. By applying the same filtering to a simulated spectrum (figure 3.12), it was estimated, that these changes hardly impair the following steps in the evaluation of our spectra. However, to keep the distortions at a minimum, we manually fine tuned the cutoff length of the rectangular window for every set of measurements.

Potential errors in the frequency domain of the spectra in a particular case are shown in figure 3.1 (enlarged image details). We found that typical deviations for the frequency value are significantly below 1 cm^{-1} for intense absorption bands. For broad and rather less intense bands at the edge of a fringe errors up to max. 1.5 cm^{-1} could be determined, which is in the range of the spectral resolution of 2 cm^{-1}. When fringes are added to the simulated spectrum in figure 3.12, the apparent maximum of the band is shifted sideways. When the FFT algorithm was applied to the simulated spectrum with added fringes in the background (figure 3.13, enlarged image details) an increase in the cutoff length and thereby removing the fringes caused a perceived shift of the maximum of the band back to the position in the undistorted spectrum. This suggests that the observed deviations in the frequency domain are not introduced by the correction itself, but by the removal of the fringes included in the original data. Therefore, the observed shifts in frequency are assumed to be towards the original value of the absorption band.
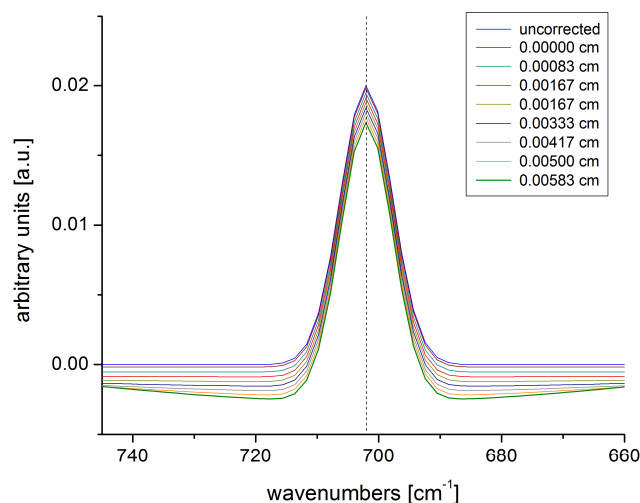
Figure 3.12. Changes in a simulated spectrum, containing only a single Gaussian band (around 700 cm^{-1}), caused by the FFT high pass filter at different cutoff lengths.
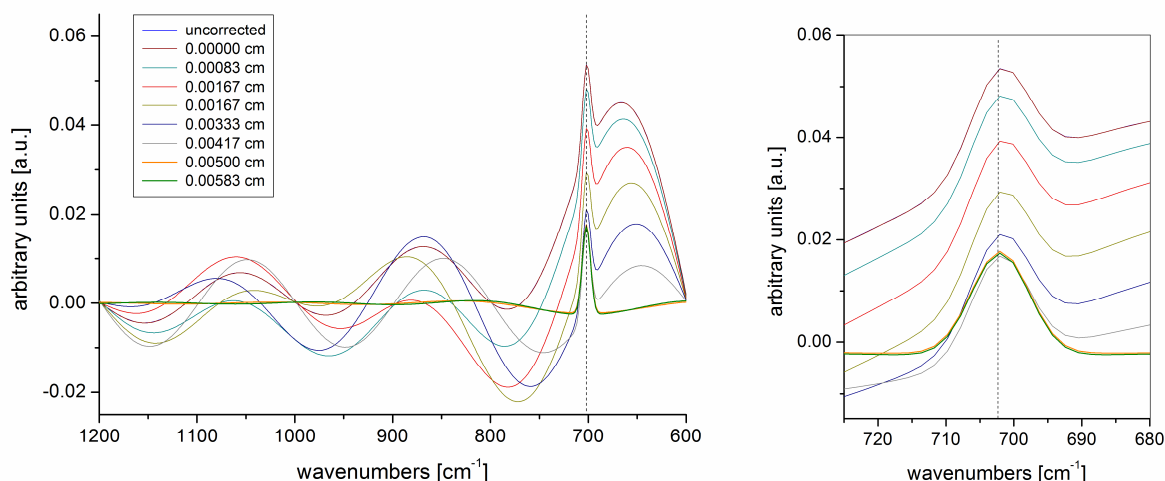
Figure 3.13. Changes in a simulated spectrum, containing the single Gaussian band shown in figure 3.12 and added fringes in the background, caused by the FFT method at different cutoff lengths. Enlarged image details (left) show the shift of the absorption band.

To visualize the effect of the FFT high pass filter on the integral of a band, the Gaussian bands in the aforementioned simulated spectra in figure 3.12 and 3.13 were integrated between 686.6 cm^{-1} and 717.5 cm^{-1} with linear background correction for a series of cutoff frequencies (see figure 3.14.; integrals normalized to the simulated band (without fringes) before applying the FFT filter). With increasing cutoff length, the integral of the band in the spectrum containing fringes moves closer to that of the band in the spectrum containing no fringes. However, as the integral of band in the spectrum without fringes also changes when the cutoff length of the filter is increased, applying the filter as little as possible is necessary.
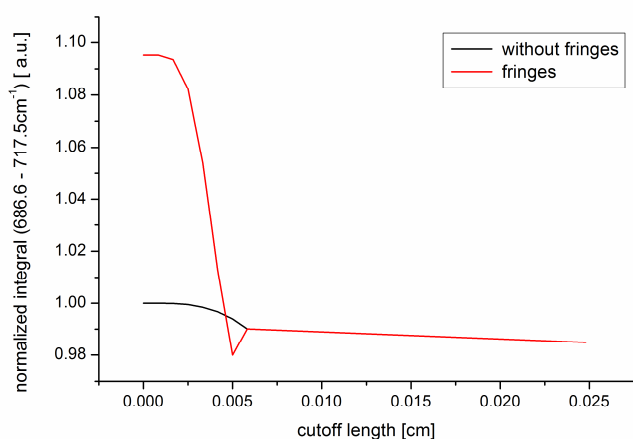
Figure 3.14. Changes of the integral of the band shown in Figure 3.12 and 3.13, normalized to the integral of the band in figure 3.12. before applying the FFT filter, with increasing cutoff length.

4. Metal Halogen Exchange on Aryl Halides

The detection of significant absorptions of phenyllithium is demonstrated in figure 4.1. The organolithium compound is formed in a metal halogen exchange reaction of bromobenzene using *n*BuLi (Et$_2$O, ambient temperature). Figure 4.1 illustrates IR spectra of all reagents introduced to or products formed during the reaction. This comparison confirms an intense absorption of phenyllithium around 706 cm^{-1}, which is in agreement with the absorption characteristics found in solutions of phenyllithium from commercial sources. Figures 4.2 shows the phenyllithium formation in a metal halogen exchange reactions in THF at -86°C using bromo- and iodobenzene, respectively.
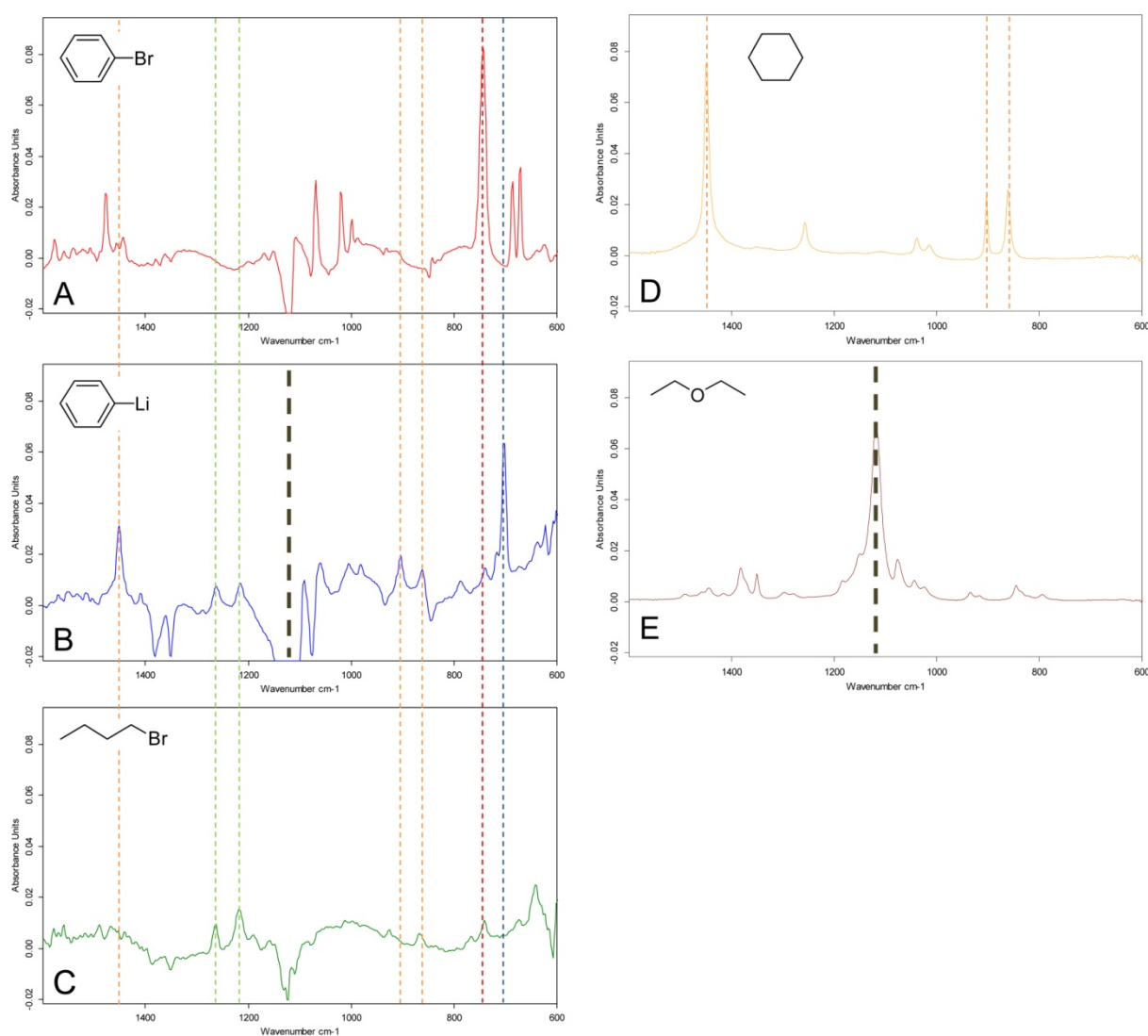
Figure 4.1. A: bromobenzene (0.25 M in Et$_2$O, background: Et$_2$O), B: phenyllithium formed in a metal halogen exchange reaction from bromobenzene using nBuLi (0.25 M in Et$_2$O, background: Et$_2$O), C: bromobenzene (0.25 M in Et$_2$O, background Et$_2$O), D: cyclohexane (background: air), E: Et$_2$O (background: air); all spectra measured *via* ATR-IR fibre optical system at ambient temperatures.
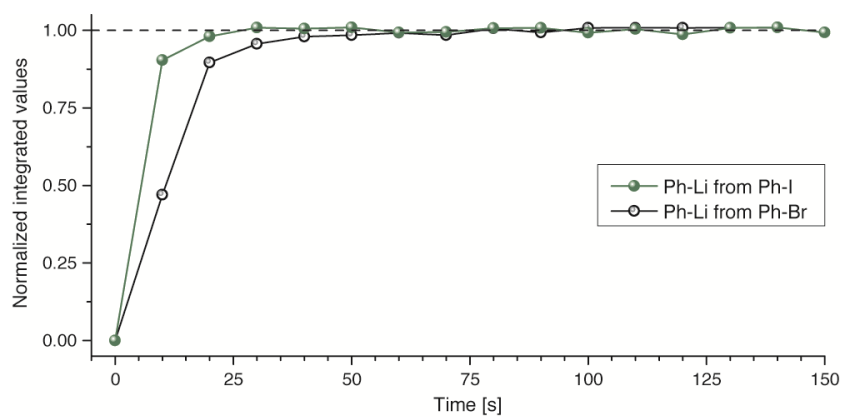
Figure 4.2. Formation of phenyllithium in a metal halogen exchange reaction of bromo- and iodobenzene (*n*BuLi, -86 °C, THF); based on integration of a characteristic IR absorption.

The results show very high reaction rates in THF at -86 °C reaching a steady state in the phenyllithium concentration within 1.0 min for bromobenzene (more spectral information is given in figures 3.1 – 3.11 in the ESI), and within 30 s when using iodobenzene.

5. Metal Halogen Exchange on Thiophene Derivatives

The accomplished metal halogen exchange reactions on thiophene derivatives proceed at very high reaction rates. During these highly exothermic reactions of 2-bromo- and 3-bromobenzene using *n*BuLi in THF at -86 °C no reliable data can be achieved as a result of large temperature deviations. To decrease the intensity of the deviations a stepwise addition of the lithiation reagent (*n*BuLi in THF) was performed. Indeed reliable spectral information could be obtained which clearly demonstrate the high formation rates for both 2-lithiumthiophen (figure 5.1) and 3-lithiumthiophene (figure 5.2).
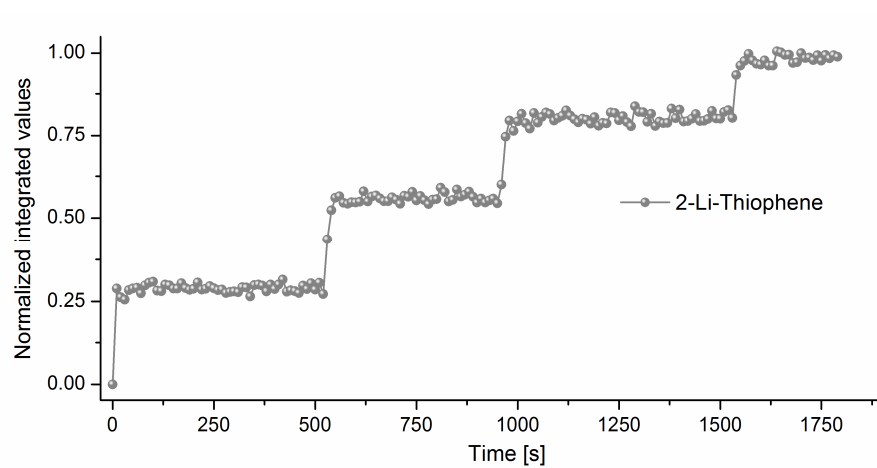
Figure 5.1. Stepwise addition experiment; formation of 2-lithiumthiophene in a metal halogen exchange reaction from 2-bromothiophene (*n*BuLi, THF, -86 °C).
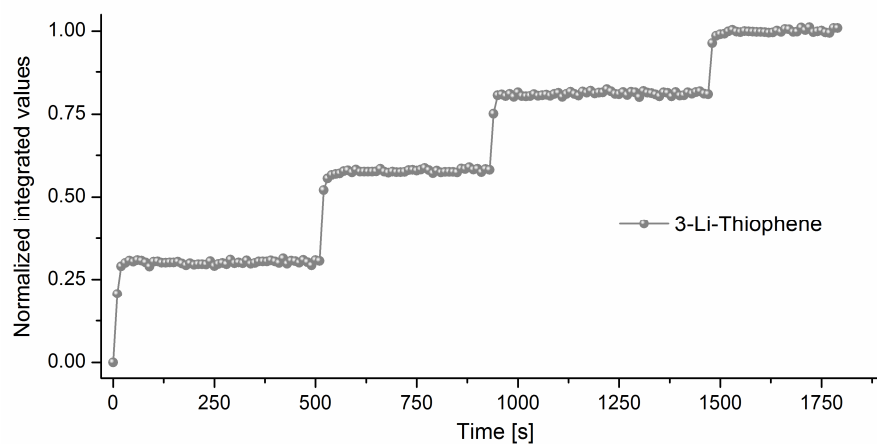
Figure 5.2. Stepwise addition experiment; formation of 3-lithiumthiophene in a metal halogen exchange reaction from 3-bromothiophene (*n*BuLi, THF, -86 °C).

6. Double-sided Halogen Dance Reaction
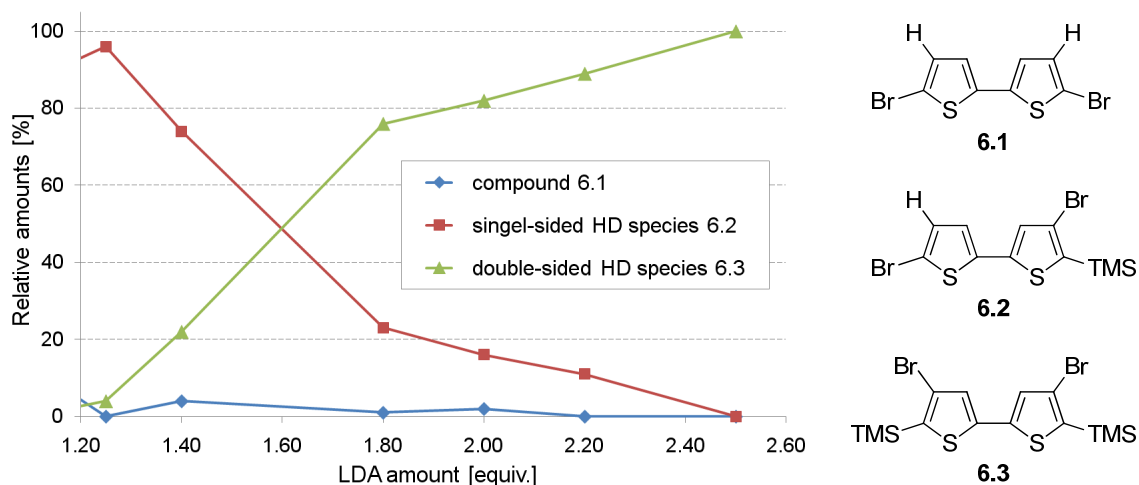
Figure 6.1. Double-sided halogen dance reaction in dependence of added LDA amount; product distribution (left), products formed during the reaction sequence (right).

Complementary to the result presented in the article we examined the ratio of single- and double-sided Halogen Dance (HD) reaction depending on the amount of Li-reagent. For this purpose the reactions were conducted at variable amounts of LDA and subsequently quenched using an excess of TMS-Cl as an electrophile. The constitution of the reaction mixture regarding **6.1**, **6.2**, and **6.3**, respectively, were investigated by NMR spectroscopy. The reactions were carried out in THF at -20 °C; subsequent to the addition of the corresponding amount of LDA to **6.1** the reaction was quenched with an excess of TMS-Cl after 25 – 30 min. The result disclose that at 1.25 equiv. LDA substrate **6.1** is completely consumed and the reaction mainly yielded in **6.2** (single-sided HD product); additionally it was shown that only a small amount of **6.3** (double-sided HD product) was formed. Increased amounts of LDA lead to increased product **6.3** yields, reaching a full conversion at 2.5 equiv. of LDA. These results point out that the metallation and subsequently a fast HD reaction are the first steps in the sequence exclusively leading to single-sided HD species **6.2**. This is in accord to the results found during in-line monitoring of the double sided HD reaction using 2.5 equiv. of LDA resulting in double-sided HD product. These results also support the assumption in Scheme 2 (main article) of the metallation being the rate determining step in this HD reaction; the migration of the halogen proceeds relatively fast (no accumulation of 3-silylthiophene and consequently 3-lithiothiophene species).

6.1. MCR-ALS Analysis

The MCR analysis was applied to the data set shown in figure 3 A of the manuscript. Firstly, an evolving factor analysis (EFA) for four components was applied to the data to determine the initial estimates needed for the MCR-ALS. Secondly, for the MCR-ALS analysis a unimodality constraint ("average" implementation, tolerance 1.1) for the concentration profiles was applied to the LDA and the intermediate **2** profile. The fit gave an R^2 of 99,89.